

Hyun Ik Park · Li-June Ming

## Mechanistic studies of the astacin-like *Serratia* metalloendopeptidase serralysin: highly active (>2000%) Co(II) and Cu(II) derivatives for further corroboration of a “metallotriad” mechanism

Received: 26 March 2001 / Accepted: 20 December 2001 / Published online: 15 February 2002  
© SBIC 2002

**Abstract** Serralysin is a bacterial Zn-endopeptidase which has been considered a virulence factor to cause tissue damage and anaphylactic response. It contains a coordinated Tyr that is unique to the astacin-like Zn enzymes. The coordinated Tyr has been proposed to play an important role in the action of this endopeptidase family. Several metal-substituted derivatives of serralysin (including  $\text{Mn}^{2+}$ ,  $\text{Co}^{2+}$ ,  $\text{Ni}^{2+}$ ,  $\text{Cu}^{2+}$ , and  $\text{Cd}^{2+}$  derivatives) are found to exhibit significant activities. Particularly, the Co- and Cu-substituted derivatives exhibit much higher activities than the native serralysin toward the hydrolysis of the tripeptide mimic benzoyl-Arg-*p*-nitroanilide, i.e., 35 and 49 times higher in  $k_{\text{cat}}$  and 33 and 26 times in  $k_{\text{cat}}/K_{\text{m}}$ , respectively. Such remarkably higher activities of metal-substituted derivatives, especially the Cu derivative, than that of the native Zn enzyme are rare in the literature, reflecting the uniqueness of this enzyme among all Zn enzymes. The significantly different  $k_{\text{cat}}$  yet similar  $K_{\text{m}}$  values among the several metal derivatives suggests that the metal center is involved in catalysis, but not necessarily in the binding of the substrate, whereas the dramatically different inhibition constants for Arg-hydroxamate binding to the metal-substituted derivatives indicates direct binding of this inhibitor to the metal center. The activity-pH profiles of serralysin and its  $\text{Co}^{2+}$  and  $\text{Cu}^{2+}$  derivatives and the optical-pH profile of Cu-serralysin have been obtained, in which the decrease in activity at higher pH values was found to be associated with a dramatic increase in the Tyr-to- $\text{Cu}^{2+}$  charge transfer transitions. This observation suggests that the binding of Tyr216 to the metal is inhibitory. A metal-centered mechanism is proposed for serralysin catalysis based on the results presented here, in which the detachment of

the coordinated Tyr and formation of a H-bond with the transition-state complex are considered essential for the stabilization of the transition state.

**Keywords** Astacin · Copper · Endopeptidase · Metalloprotease · Serralysin

### Introduction

Many zinc endopeptidases contain an extended metal-binding motif HExxHxxGxxH, comprised of the three coordinated His residues and a glutamate general base [1, 2, 3, 4]. These peptidases include the astacin family [5, 6, 7, 8], snake venom zinc endopeptidases [9], the extracellular metalloproteinases from *Serratia* [10], *Pseudomonas* [11], and *Erwinia* [12], and the matrixins [13]. The crystal structures of these peptidases reveal significant topological similarities, including the zinc-binding site and a “Met-turn” region [14], in spite of their low sequence homology. The astacin family includes a number of members [5, 6, 7, 8], such as astacin from crustacean digestive fluid [15, 16], mammalian membrane-bound meprins [17], bone morphogenetic protein-1 [18], *Drosophila* tolloid [19], and embryonic hatching proteins from the medakafish *Oryzias* [20, 21] and sea urchin [22]. The extracellular Zn endopeptidases from *Serratia*, *Pseudomonas*, and *Erwinia* are also very closely related to the astacin members in terms of the structure of their active site domain [10, 11, 12, 23, 24, 25]. The active-site  $\text{Zn}^{2+}$  in these proteases is bound to three His residues, a Tyr side chain, and a water molecule (Fig. 1).

These metallopeptidases are the only group of Zn proteins that contain a coordinated Tyr. This Tyr has been suggested to play a significant role in the action of these enzymes, in stabilizing the enzyme-substrate (ES) and the transition-state ( $\text{ES}^\ddagger$ ) complexes via H-bonding with the substrate on the basis of crystallographic [26, 27], kinetic [28], and spectroscopic studies [29]. The coordinated Tyr is also found to detach from the metal

H.I. Park · L.-J. Ming (✉)  
Department of Chemistry and Institute for Biomolecular Science,  
University of South Florida, Tampa, FL 33620-5250, USA  
E-mail: ming@chuma.cas.usf.edu  
Tel.: +1-813-9742220  
Fax: +1-813-9741733

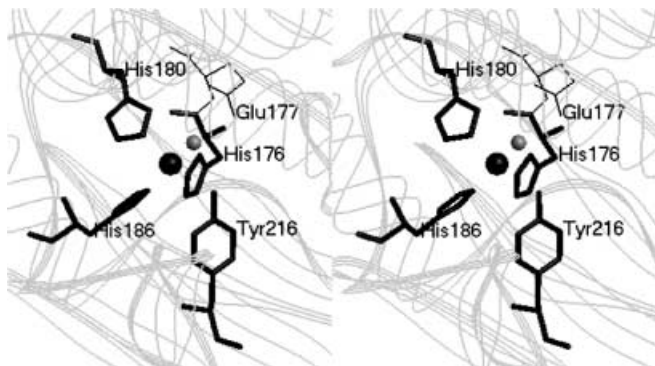


**Fig. 1.** A stereo view of the active site of serralyisin according to the crystal structure at pH 6.3 (Protein Data Bank code 1SAT; 1SRP has essentially the same structure), viewed from the top of the active-site crevice. The coordinated water molecule is shown as a *small sphere*, which is H-bonded to Glu177 and the  $O_{\eta}$  of the coordinated Tyr216. The ligands are arranged in a distorted trigonal bipyramidal geometry, in which His176, His186, and the water molecule are the equatorial ligands, and His180 and Tyr216 are the axial ligands. The distances between the  $Zn^{2+}$  and the imidazole ligands range from 2.17 Å to 2.21 Å, the water to  $Zn^{2+}$  distance is 1.95 Å, and the Tyr216( $O_{\eta}$ )-Zn bond length is 2.75 Å. Two structures of inhibitor-bound serralyisin, 1SMP and 1AF0, can also be retrieved from the PDB. The corresponding coordinated ligands in astacin (*clockwise*) are His102, His96, His92, Glu93, and Tyr149 (PDB code 1ast)

center upon inhibitor binding and forms a hydrogen bond with the inhibitor [26, 27, 29]. This might also be the case during catalysis, in which the detached Tyr is H-bonded with an oxygen of the transition-state *gem*-diolate. A recent site-directed mutagenesis study of astacin [30] showed that the substitution of an Ala for the coordinated Tyr resulted in 107 times decrease in  $k_{cat}$  but only a small change in  $K_m$  (2.7 times decrease), which demonstrated the importance of the coordinated Tyr in the action of astacin that may also be the case in other analogous enzymes such as serralyisin. However, a coordinated phenolate has been demonstrated to significantly decrease the Lewis acidity of the metal center, as reflected by the increase in the  $pK_a$  of the coordinated water ( $\geq 2$  units) above neutral pH [31, 32, 33]. Consequently, the coordinated phenolate of Tyr in the astacin-like families is supposed to be inhibitory in metal-centered hydrolysis. Nevertheless, the effective catalysis of these enzymes around neutral pH [28, 34] suggests that either the enzymes follow a metal-centered mechanism in a unique way or they may take a completely different catalytic pathway. Further investigation is thus needed to clarify the mechanism of these endopeptidases.

Bacterial endopeptidases act as virulence factors that may cause necrotic or hemorrhagic tissue damage, which in turn triggers the production of the anaphylactic and inflammatory histamine and bradykinin [35]. Serralyisin is a 50-kDa zinc endopeptidase, excreted by the opportunistic pathogen *Serratia marcescens* [36]. The structure of serralyisin consists of two domains, the N-terminal domain active site and the unique C-terminal  $\beta$ -roll

domain with seven calcium-binding sites [10]. The structure of the proteolytic domain is very similar to that of astacin [14], with the active-site zinc ion coordinated to three His residues (His176, 180, and 186), Tyr216, and a water molecule in a trigonal bipyramidal geometry (Fig. 1). The water molecule is located within hydrogen-bonding distance to Tyr216- $O_{\eta}$  and Glu177- $O_{\delta}$ . This Glu is believed to serve as a general base, analogous to Glu143 in thermolysin [37], Glu270 in carboxypeptidase A [38], and the corresponding Glu in several other metallopeptidases [39].

Our previous study of astacin has demonstrated that the highly active Co- and Cu-astacins could be used as model systems for mechanistic study of the native enzyme [29]. Therefore, metal-substituted derivatives of the astacin-like endopeptidase serralyisin are expected to be good model systems for study of the mechanism of serralyisin catalysis. Several metal ions, including  $Mn^{2+}$ ,  $Co^{2+}$ ,  $Ni^{2+}$ ,  $Cu^{2+}$ ,  $Zn^{2+}$ , and  $Cd^{2+}$ , are found to activate serralyisin to great extents. The  $Co^{2+}$  and the  $Cu^{2+}$  derivatives exhibit extraordinarily high activities toward a tripeptide mimic (33 and 26 times, respectively, higher than the native enzyme in terms of  $k_{cat}/K_m$ ), which, along with the native enzyme, have been studied by means of kinetic and optical techniques to provide further insight into the mechanism of this enzyme.

## Methods and materials

### Materials and preparation of enzyme

Metal ion solutions were prepared directly from atomic absorption standards (> 99.99%; Fisher Chemical) or from corresponding metal salts (99.95%; Sigma-Aldrich, St. Louis, Mo.) standardized against standard EDTA using xylenol orange as an indicator. All the buffers, *N*- $\alpha$ -benzoyl-L-Arg-*p*-nitroanilide (BR-*p*NA), casein, L-Arg-hydroxamate (Arg-NHOH), 1,10-phenanthroline, and EDTA were purchased from Sigma-Aldrich. Serralyisin purchased from Sigma has a purity of greater than 95% based on sodium dodecyl sulfate-polyacrylamide gel electrophoresis (SDS-PAGE), which was further purified with gel filtration (2.5 cm $\times$ 90 cm, Sephadex G-50-Fine, Sigma) to remove trace impurity, and its concentration determined according to  $A_{280}^{1\%} = 12$  [40]. The procedure for the preparation of apo-serralyisin followed that of apo-astacin [41], with the presence of 1.0 mM  $CaCl_2$  in the solutions. The activity of apo-serralyisin was consistently less than 2% of native serralyisin activity against BR-*p*NA. Metal-substituted derivatives of serralyisin were prepared by stoichiometric addition of corresponding metal ion solutions to apo enzyme in 0.02 M MES buffer at pH 6.0 in the presence of 1.0 mM  $Ca^{2+}$ . The activity of apo-serralyisin is not affected by  $Ca^{2+}$ , suggesting that  $Ca^{2+}$  is not directly involved in catalysis.

### Enzyme assays and kinetic measurements

Serralyisin favors a substrate containing at least three residues from the C-terminus [42]. It can also cleave trypsin-specific small peptides such as the tripeptide mimic BR-*p*NA, but not the dipeptides Arg-Tyr or Lys-Ala that can be hydrolyzed by trypsin [36]. For activity assay, the hydrolysis of 0.4 mM BR-*p*NA in 0.1 M HEPES buffer at pH 7.0 and 20 °C was determined on a Varian Cary 3 spectrophotometer. A 0.02 M buffer solution containing 2% DMSO and 2 mM  $Ca(NO_3)_2$  was used to avoid the precipitation of

the substrate BR-*p*NA. The presence of 2% DMSO does not affect the activity.

For kinetic studies, the hydrolytic rates of 0.15–4 mM substrate solution were determined by monitoring the release of *p*-nitroaniline at 405 nm ( $10,150 \text{ M}^{-1} \text{ cm}^{-1}$ ) in 0.1 M HEPES buffer at pH 7.0 and 30 °C in the presence of 2 mM  $\text{Ca}(\text{NO}_3)_2$ . The  $k_{\text{cat}}$  and  $K_{\text{m}}$  values were obtained by non-linear fitting of the data to the hyperbolic Michaelis-Menten equation,  $\text{rate} = k_{\text{cat}}[\text{E}_0][\text{S}]/(K_{\text{m}} + [\text{S}])$ , with  $[\text{E}_0]$  the enzyme concentration and  $[\text{S}]$  the substrate concentration. The buffers used in the pH-dependent kinetics were acetate (pH 5.0), MES (pH 5.5–6.5), HEPES (pH 7.0–8.0), TAPS (pH 8.5–9.5), and CAPS (pH 9–10). The inhibition pattern of Arg-NHOH is determined by means of Michaelis-Menten kinetics, with inhibitor concentration of 0.001–1.00 mM. For a mixed inhibition pattern [43], the specific inhibition constant  $K_{\text{ic}}$  for the dissociation of the enzyme-inhibitor complex (EI) can be obtained from the equation:

$$V_{\text{max}}^{\text{app}}/K_{\text{m}}^{\text{app}} = \frac{V_{\text{max}}/K_{\text{m}}}{1 + [\text{I}]/K_{\text{ic}}} \quad (1)$$

and the catalytic inhibition constant  $K_{\text{iu}}$  for the dissociation of the inhibitor from the enzyme-substrate-inhibitor ternary complex (ESI) is obtained according to:

$$V_{\text{max}}^{\text{app}} = V_{\text{max}}/(1 + [\text{I}]/K_{\text{iu}}) \quad (2)$$

Metal-free casein was prepared by dialyzing four times a casein solution against 1 L of 0.1 M HEPES at pH 7.0 containing 5 mM EDTA, and then four times against the buffer to remove EDTA. The initial rate of casein hydrolysis was measured according to the literature [15]. A metal-free heat-denatured casein solution (1.0%) was mixed with 0.2  $\mu\text{M}$  enzyme and incubated at 30 °C. An amount of 0.5 mL was taken every 4 min, to which 0.5 mL of 10% trichloroacetic acid was added, then followed by removal of unhydrolyzed casein precipitate with centrifugation. The control was prepared in the same way except that the enzyme was added after the acid. The absorbance at 280 nm of the supernatant was measured against the control, and fitted to a pseudo-first-order rate law to afford the observed rate constant,  $k_{\text{obs}}$ .

## Results and discussion

### Metal-substituted derivatives of serralysin

Metal substitution is a convenient method for probing the structures and catalytic mechanisms of metallopro-

teins by means of spectroscopic techniques [44]. Thus, the spectroscopically inert  $\text{Zn}^{2+}$  ion in serralysin is replaced with other metal ions for the study of this protease. All the metal ions tested, including  $\text{Co}^{2+}$ ,  $\text{Cu}^{2+}$ ,  $\text{Ni}^{2+}$ ,  $\text{Zn}^{2+}$ ,  $\text{Cd}^{2+}$ , and  $\text{Mn}^{2+}$ , can activate apo-serralysin to great extents toward the hydrolysis of BR-*p*NA and casein (Table 1). The native Zn-serralysin shows the highest pseudo-first-order activity toward casein hydrolysis (Fig. 2A). Although the activations by  $\text{Ni}^{2+}$ ,  $\text{Cd}^{2+}$ , and  $\text{Mn}^{2+}$  are much smaller than that by the native enzyme, it is still quite significant as the auto-hydrolytic rate of casein under the assay conditions is not detectable. The activities of the metal-substituted derivatives toward BR-*p*NA hydrolysis are quite significant, particularly the  $\text{Co}^{2+}$  and  $\text{Cu}^{2+}$  derivatives. The relative activities of Co- and Cu-serralysin in terms of  $k_{\text{cat}}$  and  $k_{\text{cat}}/K_{\text{m}}$  are much greater than those of any metal-substituted derivatives of Zn enzymes ever reported [44]. Moreover, their endopeptidase activities are also quite significant (81% and 13%, respectively).

The Lewis acidity of the metal ions is the key factor in metal-centered hydrolysis, in which the  $\text{p}K_{\text{a}}$  of the coordinated water is significantly lowered to assist its nucleophilic attack on the scissile bond at neutral pH. Consequently, several synthetic  $\text{Cu}^{2+}$  complexes with high Lewis acidity have been demonstrated to catalyze hydrolytic reactions [45, 46, 47]. A few  $\text{Cu}^{2+}$ -substituted Zn hydrolases, including *Aeromonas* aminopeptidase (aAP) [48], astacin [53], and serralysin, also exhibit significant activities, which further corroborates the theory. Di-Cu-aAP exhibits only 5% and 9%, respectively, activities in terms of  $k_{\text{cat}}$  and  $k_{\text{cat}}/K_{\text{m}}$  toward the hydrolysis of the specific substrate Leu-*p*NA [48], while  $\text{Cu}^{2+}$ -astacin shows 37% activity in terms of  $k_{\text{cat}}/K_{\text{m}}$  toward succinyl-tri-Ala-*p*NA hydrolysis [53]. Despite the high Lewis acidity of  $\text{Cu}^{2+}$ , almost all  $\text{Cu}^{2+}$ -substituted derivatives of Zn hydrolytic enzymes are inactive or exhibit much lower activities than the native enzymes [32, 44]. It is still not clear why  $\text{Cu}^{2+}$  cannot activate most metallohydrolases. It might be attributed to the geometric distortion of the  $\text{Cu}^{2+}$  center due to the Jahn-Teller

**Table 1.** Activation of apo serralysin<sup>a</sup> by metal ions in 0.1 M HEPES and 2 mM  $\text{Ca}(\text{NO}_3)_2$  at pH 7.0 and 30 °C

	Casein			BR- <i>p</i> NA			
	$k_{\text{obs}}$ $10^{-3} \text{ min}^{-1}$	Activity %	$K_{\text{m}}$ mM	$k_{\text{cat}}$ $\text{s}^{-1}$	$k_{\text{cat}}/K_{\text{m}}$ $\text{M}^{-1} \text{ s}^{-1}$	% Activity	
						$k_{\text{cat}}$	$k_{\text{cat}}/K_{\text{m}}$
$\text{Zn}^{2+}$	$70 \pm 3$	100	$0.65 \pm 0.05$ (0.78) <sup>b</sup>	$0.037 \pm 0.002$ (0.044) <sup>c</sup>	57	100	100
$\text{Co}^{2+}$	$57 \pm 1$	81	$0.70 \pm 0.20$ (0.88) <sup>b</sup>	$1.3 \pm 0.4$ (1.8) <sup>c</sup>	1860	3500	3300
$\text{Cu}^{2+}$	$8.9 \pm 0.3$	13	$1.2 \pm 0.5$ (0.92) <sup>b</sup>	$1.8 \pm 0.4$ (2.5) <sup>c</sup>	1500	4900	2600
$\text{Ni}^{2+}$	$4.7 \pm 0.2$	6.7	$1.67 \pm 0.12$	$0.187 \pm 0.013$	112	505	197
$\text{Cd}^{2+}$	$4.2 \pm 0.2$	6.0	$1.24 \pm 0.13$	$0.012 \pm 0.001$	9.6	32	17
$\text{Mn}^{2+}$	$2.6 \pm 0.2$	3.7	$1.44 \pm 0.13$	$0.029 \pm 0.001$	20.1	78	35

<sup>a</sup>Enzyme concentrations are 3.0, 0.50, 0.50, 0.50, 0.48, 2.4, and 2.4  $\mu\text{M}$  for  $\text{Zn}^{2+}$ ,  $\text{Co}^{2+}$ ,  $\text{Cu}^{2+}$ ,  $\text{Ni}^{2+}$ ,  $\text{Cd}^{2+}$ , and  $\text{Mn}^{2+}$  derivatives, respectively

<sup>b</sup> $K_{\text{m}}^{\text{app}}$  for substrate inhibition

<sup>c</sup> $k_{\text{cat}}^{\text{app}}$  for substrate inhibition

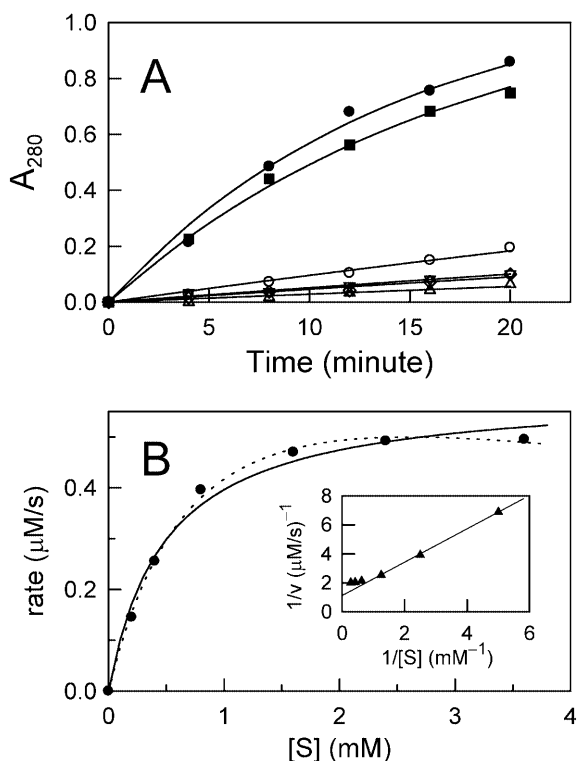


**Fig. 2.** **A** The hydrolysis of 1.0% casein by 0.20  $\mu\text{M}$  Zn-, Co-, Cu-, Ni-, Cd-, and Mn-serralyisin (from top to bottom). The solid traces are the best fits to a pseudo-first-order rate law, which afford the rate constant  $k_{\text{obs}}$  for each derivative (Table 1). **B** Fitting of BR-pNA hydrolysis by Co-serralyisin to the Michaelis-Menten kinetics (solid trace) and the best fit for a substrate inhibition pattern (dotted trace). The slight substrate inhibition pattern is also shown in the linear Lineweaver-Burk plot (inset)

effect, which can decrease the nucleophilicity of the attacking coordinated water if it is positioned at the axial positions. Unfortunately, the lack of activity hinders mechanistic study of the  $\text{Cu}^{2+}$  derivatives by means of kinetic methods. Therefore, the highly active Cu-serralyisin can serve as a prototype to gain further insight into serralyisin catalysis and to provide more information about  $\text{Cu}^{2+}$ -centered hydrolytic reactions.

Conversely, full or higher activities are usually observed for  $\text{Co}^{2+}$ -substituted derivatives of  $\text{Zn}^{2+}$  enzymes [44, 49], such as aminopeptidase [48, 50], carboxypeptidase A [51], and astacin [53]. This has been attributed to the similar coordination chemistry of  $\text{Co}^{2+}$  and  $\text{Zn}^{2+}$  [44, 49]. However, the much higher activity of  $\text{Co}^{2+}$ -serralyisin than that of the native enzyme (Table 1) is still seldom seen among all  $\text{Co}^{2+}$ -substituted Zn enzymes [44, 48, 49, 50, 51, 53]. It is worth noting that Co-serralyisin also exhibits a nearly full endopeptidase activity (81%) toward denatured casein (Fig. 1, Table 1), which justifies well its use as a mechanistic model for serralyisin action.

While the  $K_{\text{m}}$  values of the metal-substituted derivatives differ by only 2.5 fold, the  $k_{\text{cat}}$  values differ significantly by  $\sim 150$  fold (Table 1). The very different  $k_{\text{cat}}$  values reflect that the metal ion is essential in catalysis,

i.e., a metal-centered catalysis, whereas the similar  $K_{\text{m}}$  values suggest that the metal ion might not be involved in direct substrate binding other than electrostatic interactions. Similar results were previously observed for metal-substituted derivatives of carboxypeptidase A [51], in which the different  $k_{\text{cat}}$  values are indicative of the involvement of the metal center in catalysis and the similar  $K_{\text{m}}$  values in peptide hydrolysis are attributed to the lack of direct substrate binding to the metal center, whereas the significantly different  $K_{\text{m}}$  values in ester hydrolysis suggest the importance of metal in substrate binding. Since  $K_{\text{m}}$  is not the dissociation constant for substrate binding, it can only serve as a rough indicator for substrate binding.

Michaelis-Menten kinetic analysis of serralyisin catalysis reveals that the rate decreases slightly at high substrate concentrations as represented by the  $\text{Co}^{2+}$  derivative (Fig. 2B, Table 1), suggesting the possible presence of substrate inhibition [43]. In this case, the enzyme can bind a second substrate molecule  $S'$  to yield an inactive  $\text{ES-S}'$  complex with a substrate inhibition constant of  $K'_{\text{si}}$ , and the rate law becomes:  $\text{rate} = k'_{\text{cat}}[\text{S}] / (K'_{\text{m}} + [\text{S}] + [\text{S}]^2/K'_{\text{si}})$ , in which  $k'_{\text{cat}}$  and  $K'_{\text{m}}$  are the counterparts of the Michaelis-Menten parameters in substrate-inhibition kinetics [43]. The substrate inhibition is much weaker than the productive substrate binding ( $\lesssim 10$  times); thus the reaction can be approximated to follow the regular Michaelis-Menten kinetics.

#### Electronic spectra of $\text{Co}^{2+}$ - and $\text{Cu}^{2+}$ -serralyisin

Introduction of 1 equivalent of  $\text{Co}^{2+}$  or  $\text{Cu}^{2+}$  to apo-serralyisin affords the corresponding metal-substituted derivatives with characteristic electronic transitions. The electronic spectrum of  $\text{Co}^{2+}$ -serralyisin has maximum absorption at 506 nm ( $78 \text{ M}^{-1} \text{ cm}^{-1}$ ) and shoulders at ca. 470 and 530 nm (Fig. 3A), attributed to the d-d transitions of the  $\text{Co}^{2+}$  center. This spectrum is similar to that of  $\text{Co}^{2+}$ -astacin [41] with a trigonal bipyramidal geometry [53], reflecting that the  $\text{Co}^{2+}$  in serralyisin probably has the same geometry. The molar absorptivity in the range between that of a tetrahedral ( $> 150 \text{ M}^{-1} \text{ cm}^{-1}$ ) and an octahedral geometry ( $< 60 \text{ M}^{-1} \text{ cm}^{-1}$ ) [49] supports a trigonal bipyramidal geometry, although the low magnitude cannot completely exclude a distorted octahedral geometry in solution.

Three absorption bands are detected for  $\text{Cu}^{2+}$ -serralyisin between 300 and 800 nm at pH 8.8 (Fig. 3B, dashed traces). The absorption at 725 nm ( $128 \text{ M}^{-1} \text{ cm}^{-1}$ ) can be assigned to the d-d transition of the  $\text{Cu}^{2+}$  center, similar to that of  $\text{Cu}^{2+}$ -thermolysin ( $\epsilon_{730} = 90 \text{ M}^{-1} \text{ cm}^{-1}$ ) with a tetragonally distorted  $\text{Cu}^{2+}$  center [52]. The transitions at 320 and 454 nm with much higher intensities of 1070 and  $1283 \text{ M}^{-1} \text{ cm}^{-1}$ , respectively, are due to tyrosinate-to- $\text{Cu}^{2+}$  charge transfer (CT) transitions as observed in Cu-astacin at 325 and 445 ( $1900 \text{ M}^{-1} \text{ cm}^{-1}$ ) nm [53]. In the crystal structure of  $\text{Cu}^{2+}$ -astacin, the  $\text{Cu}^{2+}$  center retains a distorted

trigonal bipyramidal geometry as in the native enzyme [53] (cf. Fig. 1). However, the EPR spectrum of  $\text{Cu}^{2+}$ -astacin in frozen solution exhibits  $g_{\parallel} > g_{\perp}$  features,

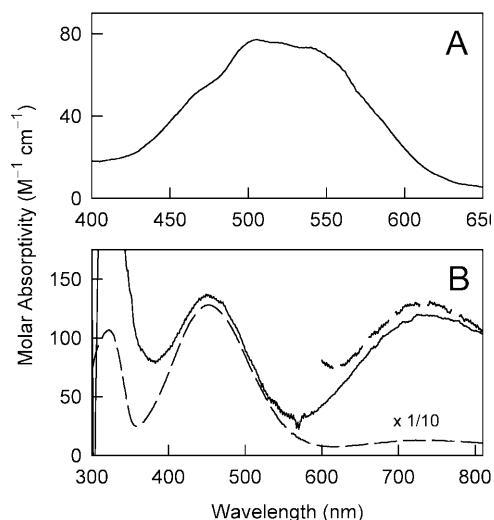


**Fig. 3.** The electronic spectra (Varian Cary 3E) of serralysin (0.20–0.65 mM) in 20 mM MES buffer at pH 5.5 in the presence of 2 mM  $\text{Ca}(\text{NO}_3)_2$  upon binding of 1 equiv  $\text{Co}^{2+}$  (A) and  $\text{Cu}^{2+}$  (B) and referenced against apo-serralysin. There is no change in the spectra with more than 1 equiv metal ion added. The dashed trace in B is the spectrum obtained in 20 mM TAPS buffer at pH 8.8

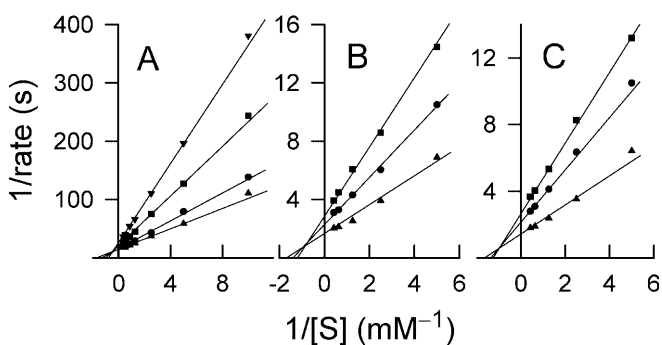


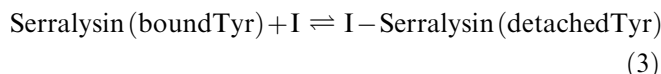
**Fig. 4.** Arg-NHOH inhibition of A 2.4- $\mu\text{M}$  Zn-, B 0.48- $\mu\text{M}$  Co-, and C 0.48- $\mu\text{M}$  Cu-serralysin at pH 7.0 in 0.1 M HEPES buffer in the presence of 2 mM  $\text{Ca}(\text{NO}_3)_2$  expressed as the Lineweaver-Burk plots. The inhibitor concentrations are 0.0, 0.2, 0.8, and 1.6 mM in A, 0.0, 5.0, and 10.0  $\mu\text{M}$  in B, and 0.0, 1.25, and 2.50  $\mu\text{M}$  in C. The kinetic parameters  $k_{\text{cat}}$  and  $K_{\text{m}}$  are obtained from direct fitting of the data to the Michaelis-Menten equation, from which the specific inhibition constant  $K_{\text{ic}}$  and the catalytic inhibition constant  $K_{\text{iu}}$  are obtained (Table 2)

suggesting a tetragonally distorted  $\text{Cu}^{2+}$  coordination sphere in solution or a very weak axial ligand field [29, 53]. Our preliminary study of Cu-serralysin also revealed  $g_{\parallel} > g_{\perp}$  features, suggesting a tetragonally distorted  $\text{Cu}^{2+}$  center (Park HI, Angerhofer A, Ming L-J, unpublished observations).

### Inhibition by L-Arg-hydroxamate

The inhibitions of  $\text{Zn}^{2+}$ -,  $\text{Co}^{2+}$ -, and  $\text{Cu}^{2+}$ -serralysin by the metal chelating inhibitor L-Arg-hydroxamate (Arg-NHOH) at pH 7.0 display a mixed pattern (Fig. 4) with significantly different inhibition constants  $K_{\text{ic}}$  and  $K_{\text{iu}}$  (Table 2), whereas their  $K_{\text{m}}$  values for the hydrolysis of BR-*p*NA are very close to each other (Table 1). These results indicate that while the substrate does not seem to bind to the metal center, the inhibitor binds directly to the metal ion. A recent crystallographic study of inhibitor binding of serralysin showed that the inhibitor Leu-Ala-hydroxamate is bound directly to the active-site metal (Baumann U, unpublished results, with the structure deposited in the Protein Data Bank, PDB code 1af0). The observation of a mixed inhibition pattern and substrate inhibition suggests the presence of an alternative site for inhibitor and the substrate binding in the ES complex to form the ES-I and ES-S ternary complexes, respectively.

The CT transition in  $\text{Cu}^{2+}$ -serralysin at 454 nm can serve as an indicator for the metal-binding status of Tyr216. Upon addition of 1 equivalent of Arg-NHOH to Cu-serralysin at pH 5.5, the weak charge transfer transition is abolished nearly completely whereas the d-d transition is intact. However, the decrease in the CT intensity upon the addition of the inhibitor is less dramatic at pH 8.8, along with a very small shift of the d-d transition to 720 nm (Fig. 5). The results indicate that the coordinated Tyr is detached upon inhibitor binding, as observed in a previous study of Cu-astacin [29]. The gradual decrease in the CT intensity at pH 8.8 upon inhibitor binding can be described by the following equilibrium:



with the assumption that the binding of one inhibitor molecule (I) to the metal results in a concomitant detachment of the coordinated Tyr. The binding of any

**Table 2.** Ionization constants from pH profiles of  $k_{\text{cat}}/K_{\text{m}}$  and  $k_{\text{cat}}$  of Zn-, Co-, and Cu-serralysin and inhibition constants of Arg-NHOH for the hydrolysis of BR-*p*NA in 0.1 M HEPES buffer and 2 mM  $\text{Ca}(\text{NO}_3)_2$  at pH 7.0 and 30 °C

	$k_{\text{cat}}$			$k_{\text{cat}}/K_{\text{m}}$			Inhibition constants		
	$k_{\text{lim}}$ ( $\text{s}^{-1}$ )	$\text{p}K_{\text{a1}}$	$\text{p}K_{\text{a2}}$	$k_{\text{lim}}$ ( $\text{M}^{-1} \text{s}^{-1}$ )	$\text{p}K_{\text{a1}}$	$\text{p}K_{\text{a2}}$	$K_{\text{ic}}$ ( $\mu\text{M}$ )	$K_{\text{iu}}$ ( $\mu\text{M}$ )	$K_{\text{si}}$ (mM)
Zn	$0.040 \pm 0.003$	$5.33 \pm 0.18$	$9.09 \pm 0.17$	$59.0 \pm 4.0$	$5.74 \pm 0.14$	$8.94 \pm 0.14$	$560 \pm 10$	$2570 \pm 230$	19
Co	$1.71 \pm 0.13$	$6.41 \pm 0.14$	$9.20 \pm 0.15$	$1700 \pm 90$	$6.20 \pm 0.11$	$9.09 \pm 0.11$	$7.57 \pm 0.02$	$10.4 \pm 0.3$	7.7
Cu	$2.8 \pm 0.3$	$5.97 \pm 0.14$	$7.74 \pm 0.13$	$2130 \pm 200$	$6.30 \pm 0.07$	$7.32 \pm 0.07$	$1.40 \pm 0.12$	$2.79 \pm 0.14$	8.5

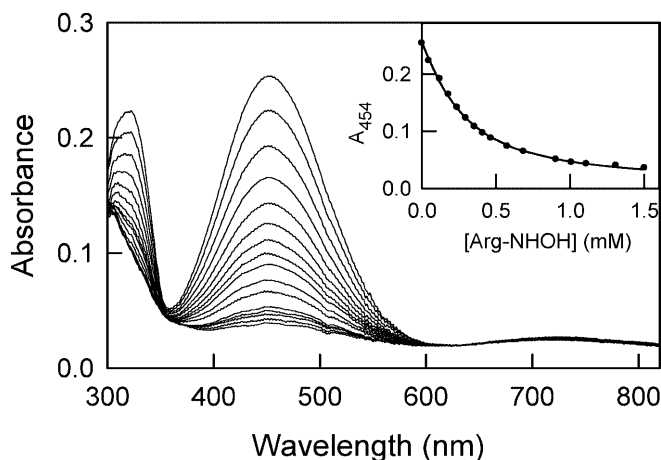


**Fig. 5.** Titration of 0.20 mM Cu-serralyisin at pH 8.8 with Arg-NHOH (from top to bottom: 0, 0.25, 0.5, 0.75, 1.0, 1.25, 1.50, 1.75, 2.0, 2.5, 3.0, 3.5, 4.0, 4.5, 5.0, 6.0, and 7.0 equivalents). The spectra were referenced against the apo-serralyisin spectrum under the same conditions. The inset shows the change in the absorption intensity at 454 nm with an increasing amount of Arg-NHOH. The solid trace is the best fit of the absorption at 454 nm to Eq. 3, which gives an apparent association constant  $K_{app} = 5.6 \times 10^3 \text{ M}^{-1}$ . Addition of 1 equiv of Arg-NHOH to Cu-serralyisin at pH 5.5 (Fig. 3B) completely abolishes the CT transitions, but the d-d transition remains intact

other Arg-NHOH molecule to the enzyme that does not displace the Tyr, if it existed, would not influence the CT transitions. A fitting of the CT intensity with respect to inhibitor concentration according to the equilibrium without including  $[\text{H}^+]$  gives an apparent association constant of  $5.6 \times 10^3 \text{ M}^{-1}$  for Arg-NHOH binding to  $\text{Cu}^{2+}$ -serralyisin at pH 8.8 (Fig. 5, inset). The pH influence on Tyr binding can be further corroborated by comparing the binding of Arg-NHOH at pH 8.8 with that in inhibition study at pH 7.0. The specific inhibition constant  $K_{ic}$  at pH 7.0 can be converted into an apparent association constant of  $7.1 \times 10^5 \text{ M}^{-1}$ . The value is much higher than that at pH 8.8, indicating that protonation of Tyr216 at lower pH assists the binding of the inhibitor Arg-NHOH.

#### pH dependence of the activities of Zn-, Co-, and Cu-serralyisin

The kinetic parameters  $K_m$  and  $k_{cat}$  for Zn-, Co-, and Cu-serralyisin toward BR-pNA hydrolysis were determined within pH 5.0–10.0. Plots of  $k_{cat}/K_m$  and  $k_{cat}$  versus pH exhibit bell-shaped curves for all derivatives (Fig. 6), indicating the involvement of at least two ionizable groups in the action of serralyisin. The data are fitted to a two-ionization process [43, 54, 55] to give two ionization constants,  $\text{p}K_{a1}$  and  $\text{p}K_{a2}$ , and the intrinsic pH-independent rate constant  $k_{lim}$  (Table 2 and Fig. 6). The coordination spheres of the  $\text{Zn}^{2+}$ ,  $\text{Co}^{2+}$ , and  $\text{Cu}^{2+}$  derivatives in the crystal structures of the analogous enzyme astacin are very similar [53], which suggests that

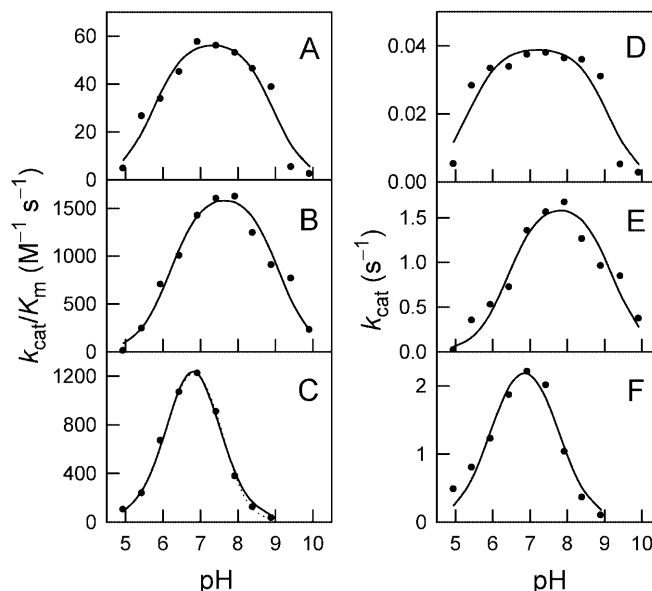


**Fig. 6.** pH dependence of  $k_{cat}$  and  $k_{cat}/K_m$  for the hydrolysis of BR-pNA by Zn- (A and D), Co- (B and E), and Cu-serralyisin (C and F). The solid lines are the best fits to the equation  $k = k_{lim} / \left(1 + \frac{[\text{H}^+]}{K_{a1}}\right) \left(1 + \frac{K_{a2}}{[\text{H}^+]}\right)$  to afford the two  $\text{p}K_a$  values reported in Table 2 for  $k = k_{cat}$  or  $k_{cat}/K_m$ . The  $k_{cat}/K_m$ -pH profile of Cu-serralyisin can also be reasonably fitted to a three-ionization process (dotted)

the difference in  $\text{p}K_a$  values of the three metal derivatives of serralyisin is possibly attributable to their different Lewis acidities, but not due to a significant structural change in the coordination sphere.

The low  $\text{p}K_{a2}$  approaching  $\text{p}K_{a1}$  seriously affects the activity of Cu-serralyisin, causing a dramatic decrease in maximum activity, i.e.,  $k_{cat}/K_m$  decreases from the intrinsic maximum value of 2130 to the fitted maximum value of  $1220 \text{ M}^{-1} \text{ cm}^{-1}$  at pH 7.0, whereas the values for Zn- and for Co-serralyisin are not significantly changed (i.e., 60 versus 57 and 1700 versus  $1420 \text{ M}^{-1} \text{ cm}^{-1}$ , respectively; Table 2 and Fig. 6). In this situation, only 57% Cu-serralyisin is active, which makes this derivative much more efficient than the native enzyme (i.e.,  $k_{cat}/K_m$  of Cu-serralyisin becomes 46 times higher than that of the native enzyme in terms of the active form of the enzyme). The sharp decrease in  $k_{cat}$  of Cu-serralyisin at high pH suggests the possibility of another ionization. A fitting of the data to a three-ionization process gives  $\text{p}K_a$  values of  $6.19 \pm 0.05$ ,  $7.51 \pm 0.07$ , and  $8.40 \pm 0.24$ , and  $k_{lim} = 1780 \pm 90 \text{ M}^{-1} \text{ s}^{-1}$  (Fig. 6C, dotted trace).

For the ionizable groups to be influenced by the metal ion, they must be either located very close to or coordinated to the metal ion. Hence, the best candidates are Tyr216, the metal-bound water, and Glu177 that is H-bonded to the coordinated water (Fig. 1). Such a “metallotriad” framework of  $\text{M}-\text{OH}\cdots\text{OOC}-$  is analogous to the triad  $\text{Ser}-\text{OH}\cdots\text{His}\cdots\text{OOC}-$  in serine hydrolases, with the nucleophile sandwiched by a Lewis acid (M) and a Lewis base (carboxylate). This “metallotriad” framework has been demonstrated to

effectively increase the nucleophilicity of the coordinated water in metallohydrolases [39], including thermolysin [37], matrilysin [56, 57], and carboxypeptidase A [38]. However, some previous studies [58, 59] suggested that a general base (e.g., Tyr216 in serralyisin [28]), instead of the metal center, in the active site might serve to activate a non-coordinated water molecule for nucleophilic attack following a reverse protonation process [54, 55], i.e., the  $pK_{a1}$  of the general base is greater than the  $pK_{a2}$  of the general acid (cf. Fig. 7). The very narrow activity-pH profiles of Cu-serralyisin (Fig. 6C, D) suggest a possible presence of a reverse protonation process [60].

According to the discussion above, there are four possible ways for the assignment of the general base ( $pK_{a1}$ ) and acid ( $pK_{a2}$ ) associated with the increase and

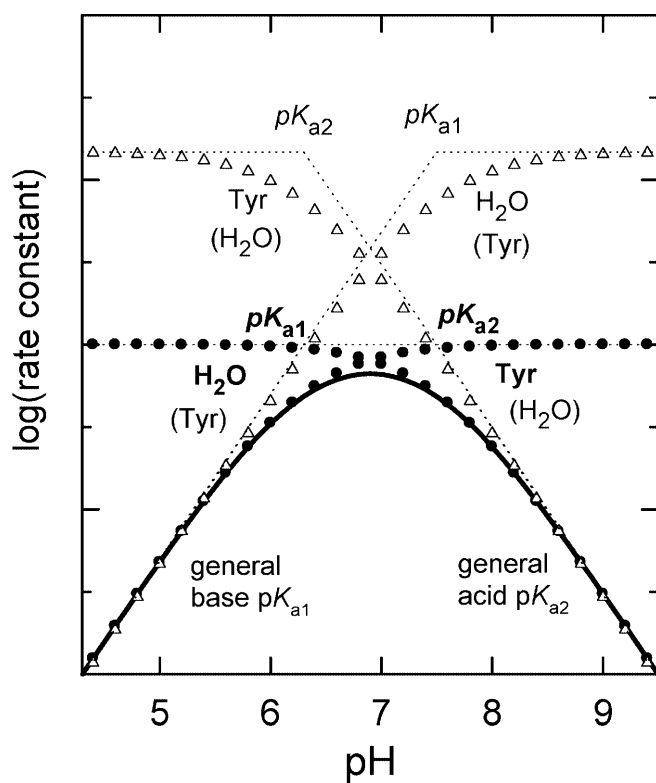


**Fig. 7.** Schematic presentation of the four possible roles of the coordinated water and Tyr216 in pH-dependent activity of serralyisin with four different assignments in which Tyr216 is assigned to be (from top to bottom) the general acid and base in a reverse protonation process, and the general acid and base in a normal protonation process. The pH-activity profile (solid curve) has been deconvoluted to show the general base whose deprotonation enhances the activity and the general acid whose deprotonation decreases the activity in a normal protonation process with  $pK_{a2} > pK_{a1}$  (filled circles) and a reverse protonation process with  $pK_{a1} > pK_{a2}$  (open triangles). The second and the fourth assignments (from the top) are excluded by mutagenesis studies of the analogous astacin and the first and the fourth assignments are excluded based on optical and crystallographic studies, which leave the only possible assignment to be the third assignment in which the coordinated water and Tyr216 serve as the general base and acid associated with  $pK_{a1}$  and  $pK_{a2}$ , respectively, in a normal protonation process (bold labels). Note that the intrinsic rate constant  $k_{\text{lim}}$  is much larger in the case of a reverse protonation process

decrease in activity, respectively, as represented by the simulated trace in Fig. 7 (solid trace), with the coordinated water serving as the nucleophile (associated with  $pK_{a1}$ ) or Tyr216 being the general base (labeled in parentheses) in either a normal protonation process (filled circles) or a reverse protonation process (open triangles). The deprotonation of Tyr216 and its coordination to the metal is considered inhibitory when water serves as the nucleophile.

The  $pK_{a1}$  values are close to those found for the coordinated water in the “metallotriad” of carboxypeptidase A and its  $\text{Co}^{2+}$  derivative, i.e., 6.3 and 5.6, respectively [61], and thermolysin (5.1) [62], suggesting the  $pK_{a1}$  in serralyisin is possibly attributable to the coordinated water. However, the  $pK_a$  of a coordinated water is significantly increased by about three units (may reach  $>10$ ) in  $\text{Zn}^{2+}$  and  $\text{Co}^{2+}$  complexes when a coordinated phenolate group is present [29, 31, 32, 33]. From these studies, it seems consistent, *yet not conclusive*, to assign  $pK_{a1}$  to the phenol group of Tyr216 and  $pK_{a2}$  to a coordinated water, as proposed in the previous study [28].

The recent study of the Tyr149→Phe and the Glu93→Ala mutants of the analogous astacin shows that the coordinated Tyr149 is not indispensable for catalysis, whereas Glu93 is [30]. The  $\sim 100$ -fold decrease in  $k_{\text{cat}}$  for the mutant Y149F is equivalent to  $\sim 12 \text{ kJ mol}^{-1}$  increase in the Gibbs free energy of activation at 303 K, which can be due to the loss of one H-bonding stabilization. The lack of activity in the E93A mutant demonstrates the importance of Glu93 in the “metallotriad” in activation and orientation of the nucleophilic coordinated water in astacin. The coordinated Tyr should be indispensable if it was serving as the water-activating general base; however, this is not the case. Taking into consideration the structural similarity between serralyisin and astacin, the general base with  $K_{a1}$  cannot be assigned to Tyr216 in serralyisin in either a normal or a reverse protonation process. In order to gain further insight into the mechanism, it is important to assign the ionization constants. Thus, the  $pK_a$  values have been further investigated by monitoring the pH-dependent change of the Tyr-to- $\text{Cu}^{2+}$  CT transitions in Cu-serralyisin.

#### pH dependence of CT transitions in Cu-serralyisin

The CT transitions do not exhibit full intensities at neutral and lower pH values ( $\sim 135\text{--}500$  versus  $1400 \text{ M}^{-1} \text{ cm}^{-1}$ ) (Figs. 3B and 8), indicating that they are pH dependent. The Tyr(phenolate)-to- $\text{Cu}^{2+}$  CT transitions in Cu-serralyisin changes with pH in a sigmoidal manner (Fig. 8). Thus, the change can be described by a single-ionization process expressed in Eqs. 4 and 5 for Tyr216 ionization and simultaneous binding to the active site  $\text{Cu}^{2+}$ :

$$\varepsilon = \varepsilon_u + \varepsilon_b f_b \quad (4)$$

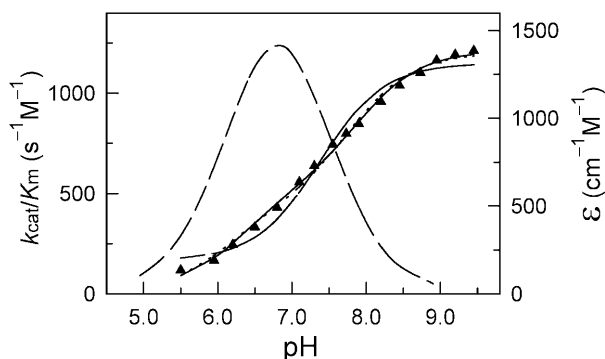


**Fig. 8.** The change in the intensity of the CT transition of Cu-serralysin at 454 nm with pH. The fitting of the sigmoidal profile to a single deprotonation process gives a poor fit (Eq. 4, *dashed trace*). The data can be much better fitted to a two-ionization process (Eq. 6, *solid trace*) or a two-ionization process in the presence of a tautomerism (Eq. 11, *dotted lines*). The *dashed bell-shaped curve* is the best fit for the  $k_{\text{cat}}/K_{\text{m}}$ -pH profile of Cu-serralysin from Fig. 6C

$$\text{pH} = \text{p}K_{\text{a}} + \log\left(\frac{f_{\text{b}}}{1 - f_{\text{b}}}\right) \quad (5)$$

where  $\epsilon_{\text{u}}$  and  $\epsilon_{\text{b}}$  are the molar absorptivities at 454 nm due to the background and the Cu-bound Tyr, respectively, and  $f_{\text{b}}$  is the mole fraction of the bound form of Tyr216. The fitting gives  $\epsilon_{\text{u}} = 189$  and  $\epsilon_{\text{b}} = 1125 \text{ M}^{-1} \text{ cm}^{-1}$ , and a  $\text{p}K_{\text{a}}$  value of 7.41 for the deprotonation of Tyr216. However, the data do not fit well to this single-ionization model (Fig. 8, *dashed trace*).

Since the side chain of Tyr216 is H-bonded to the coordinated water [10, 24, 25], its deprotonation and binding to the metal should be affected by the ionization of the coordinated water and reflected by its CT intensity. The data are indeed better fitted to a two-ionization process described by Eqs. 6, 7, 8, 9 with a fixed  $\text{p}K_{\text{a}1} = 6.30$  (consistent with that in the pH profile of  $k_{\text{cat}}/K_{\text{m}}$ ) to afford  $\text{p}K_{\text{a}2} = 7.90 \pm 0.06$ ,  $\epsilon_{\text{u}} = 24 \pm 25$ ,  $\epsilon_{\text{w}} = 580 \pm 50$ , and  $\epsilon_{\text{b}} = 1360 \pm 30 \text{ M}^{-1} \text{ cm}^{-1}$  (Fig. 7, *solid trace*), in which  $f_{\text{u}}$ ,  $f_{\text{w}}$ , and  $f_{\text{b}}$  are the mole fractions of the unbound, first deprotonated form, and the Tyr-bound form, respectively. The magnitude of the change in molar absorptivity associated with  $\text{p}K_{\text{a}1}$  is only half of that associated with  $\text{p}K_{\text{a}2}$  (i.e., 500 versus 1000). Since  $\text{p}K_{\text{a}2}$  is associated with a more pronounced change, it seems more reasonable to be assigned to the ionization of Tyr216 and binding to the  $\text{Cu}^{2+}$  center:

$$\epsilon = \epsilon_{\text{u}} + \epsilon_{\text{w}}f_{\text{w}} + \epsilon_{\text{b}}f_{\text{b}} \quad (6)$$

$$f_{\text{u}} + f_{\text{w}} + f_{\text{b}} = 1 \quad (7)$$

$$\text{pH} = \text{p}K_{\text{a}1} + \log\left(\frac{f_{\text{w}}}{f_{\text{u}}}\right) \quad (8)$$

$$\text{pH} = \text{p}K_{\text{a}2} + \log\left(\frac{f_{\text{b}}}{f_{\text{w}}}\right) \quad (9)$$

Since the  $\text{p}K_{\text{a}}$  values observed from the pH dependence of  $k_{\text{cat}}/K_{\text{m}}$  may reflect the  $\text{p}K_{\text{a}}$  values of

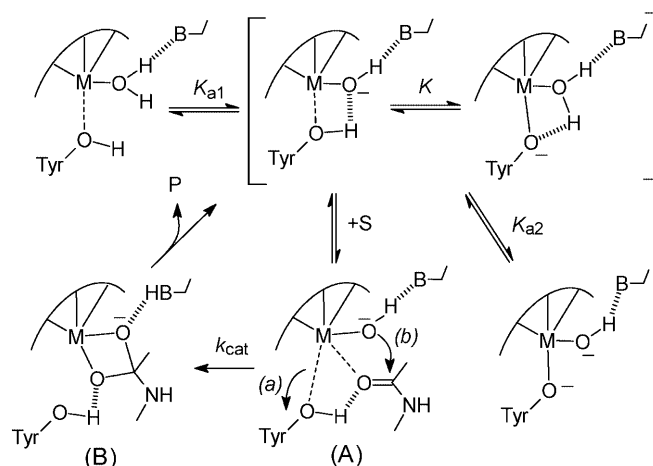
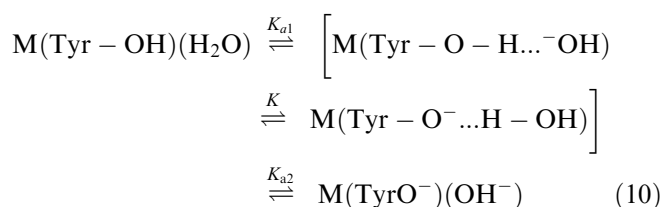


**Fig. 9.** A proposed metal-centered “metallotriad” mechanism for serralysin catalysis. In this mechanism the deprotonation of the coordinated water (associated with  $K_{\text{a}1}$ ) activates the enzyme, whereas the deprotonation of Tyr216 and its binding to the metal center (associated with  $K_{\text{a}2}$ ) are considered non-productive. The *dotted lines* represent possible electrostatic interactions, and the *ladder lines* indicate hydrogen bonds. The  $\text{Zn-O}_{\text{r}}(\text{Tyr})$  distance of 2.75 Å at pH 6.3 (above  $\text{p}K_{\text{a}1}$  but below  $\text{p}K_{\text{a}2}$ ) may represent a very weak coordination bond

the free enzyme and/or the substrate [43, 54, 55, 63], they are thus comparable to those obtained from the pH profile of the CT transitions (Fig. 8). The averaged  $\text{p}K_{\text{a}}$  of 7.41 from the one- $\text{p}K_{\text{a}}$  fitting and the second ionization constant of  $\text{p}K_{\text{a}} = 7.9$  from the two- $\text{p}K_{\text{a}}$  fitting in the optical study are more consistent with  $\text{p}K_{\text{a}2}$  (7.32 and 7.51) rather than  $\text{p}K_{\text{a}1}$  (6.30) in the pH profile of  $k_{\text{cat}}/K_{\text{m}}$ . Although the data can be reasonably fitted to the above two-ionization process, the similar  $\lambda_{\text{max}}$  throughout the titration suggests that it is likely to have only one species that affords the CT instead of two.

The presence of a H-bond between the coordinated water and Tyr216 [10, 25] in the crystal structures suggests that the deprotonation of the coordinated water may affect the CT transitions via a tautomeric equilibrium ( $K$ ) with Tyr216, as shown below (cf. Fig. 9):



Fitting of the absorptivity-pH profile to the two-ionization process in the presence of the tautomerism with a fixed  $\text{p}K_{\text{a}1} = 6.30$  and an assumption that the only chromophore is the coordinated Tyr ( $\epsilon_{\text{b}}$ ) gives  $\text{p}K_{\text{a}2} = 7.58 \pm 0.05$ ,  $K = 0.59 \pm 0.09$ , and  $\epsilon_{\text{u}} = 0 \pm 43$  (background) and  $\epsilon_{\text{b}} = 1370 \pm 50 \text{ M}^{-1} \text{ cm}^{-1}$  (Fig. 8, *dotted trace*). In this fitting, Eq. 6 is replaced with Eq. 11:

$$\varepsilon = \varepsilon_u + \varepsilon_b \left[ \frac{K}{1 + K + 1/a + b} + \frac{1}{1 + 1/b + K/b + 1/ab} \right] \quad (11)$$

in which  $a = 10^{\text{pH}-\text{p}K_{a1}}$  and  $b = 10^{\text{pH}-\text{p}K_{a2}}$ . The  $\text{p}K_{a2}$  value of 7.58 is close to the  $\text{p}K_{a2}$  obtained in the activity-pH profiles. In this case, the change in CT intensity associated with  $\text{p}K_{a2}$  is 2.4 times larger than that with  $\text{p}K_{a1}$ , consistent with the assignment of  $\text{p}K_{a2}$  to Tyr216. The ionization of Tyr and concomitant binding to the metal ion are thus considered to contribute to the decrease in activity at higher pH values. The CT intensity is slightly influenced by the ionization of  $\text{p}K_{a1}$ , suggesting that this ionization cannot be due to the remote non-coordinating Glu since it has no direct interaction with Tyr216 to affect the CT. The crystal structure of Zn-serralyisin at pH 6.3 (a value greater than  $\text{p}K_{a1}$  and less than  $\text{p}K_{a2}$ ) reveals a short Zn-water distance of 1.95 Å and a long Zn-Tyr216 distance of 2.75 Å [10]. These bond lengths are consistent with a deprotonated water and a protonated Tyr216 at pH 6.3, thus excluding the assignment of  $\text{p}K_{a2}$  to the coordinated water in normal protonation process or  $\text{p}K_{a1}$  to the water in reverse protonation process, which is also consistent with our assignment. Combining the studies described above with the mutagenesis studies of the analogous astacin [30] and the crystal structure of serralyisin, the only possible assignment is that  $\text{p}K_{a1}$  and  $\text{p}K_{a2}$  are associated with the coordinated water and Tyr216, respectively, in a normal protonation process (bold labels in Fig. 7).

The close relationship between the coordinated water and the coordinated Tyr216 is also shown by comparing the different metal derivatives of serralyisin and the analogous astacin. The shorter metal-( $\text{O}_\eta$ )Tyr bond length of 2.10 Å in the analogous Cu-astacin than that in Zn-astacin (2.54 Å) [53] and the stronger Lewis acidity of  $\text{Cu}^{2+}$  than that of  $\text{Zn}^{2+}$  suggest that the Tyr in the  $\text{Cu}^{2+}$  derivative should exhibit a lower  $\text{p}K_a$  than that in the  $\text{Zn}^{2+}$  derivative. The stronger binding of the negatively charged Tyr to the metal center should decrease the Lewis acidity of the metal center, which should result in a significant increase in the  $\text{p}K_a$  value of the coordinated water, as observed in the studies of metal complexes [31, 32, 33]. Therefore, the higher  $\text{p}K_{a1}$  and lower  $\text{p}K_{a2}$  values in Cu-serralyisin relative to those in Zn-serralyisin (Table 2) are also consistent with the assignment of  $\text{p}K_{a1}$  and  $\text{p}K_{a2}$  to the coordinated water and Tyr216, respectively. Since the difference in the  $\text{p}K_a$  values between Zn- and Co-serralyisin is not as dramatic, such analysis was not attempted for these two derivatives.

### Mechanism for serralyisin

A recent study of  $\text{Zn}^{2+}$ -serralyisin suggests that the coordinated Tyr216 (assigned to a  $\text{p}K_{a1}$  of 4.8) serves as the general base [28]. The coordinated water is proposed

to be displaced upon substrate binding. This displaced water or a solvent water molecule is activated by the coordinated Tyr216 via a H-bonding interaction with the phenolate  $\text{O}_\eta$ , then followed by nucleophilic attack on the scissile bond. The decrease in activity at high pH was attributed to the deprotonation of a coordinated His residue or formation of a “non-displaceable  $\text{Zn}(\text{II})\text{-OH}^-$ ”. Although this mechanism seems consistent with the experimental observations, it can be challenged by the facts that (1) the very acidic coordinated Tyr216 yields  $\text{O}_\eta^-$  with a low Lewis basicity which may not effectively activate a water to perform nucleophilic attack; (2) the  $\text{Zn}^{2+}$ -coordinated  $\text{OH}^-$  is not difficult to be displaced as  $\text{Zn}^{2+}$  is kinetically labile; (3) the coordinated Tyr is displaced by transition-state analogues and inhibitors [26, 27, 29], which might also be the case during catalysis; (4) the two ionization constants  $\text{p}K_{a1}$  and  $\text{p}K_{a2}$  are best assigned to the coordinated water and Tyr216, respectively, in a normal protonation process according to our study presented here.

A metal-centered mechanism (described in Fig. 9) is thus proposed for the action of serralyisin. In this mechanism, the deprotonation of the coordinated water accounts for the increase in activity, whereas the deprotonation of Tyr216 and its coordination to the metal are believed to be inhibitory. The deprotonation of the coordinated water (with  $\text{p}K_{a1}$ ) to form the active enzyme is further assisted by the general base Glu177 via the “metallotriad” framework (Fig. 9, top structures). An electrostatic interaction of the scissile peptidyl carbonyl of the substrate with the active site metal may enhance the polarity of the carbonyl group for nucleophilic attack, which may be associated with a partial breakage of the metal-Tyr216 interaction to afford a pseudo-six-coordinate transient state (A in Fig. 9). The expansion of the coordination sphere of the active-site metal may accommodate steric crowding generated by substrate binding, which has been suggested to occur in carboxypeptidase A [38, 64, 65, 66, 67], thermolysin [37], and collagenase [68, 69]. Since  $\text{Cu}^{2+}$  prefers a tetragonally distorted octahedral coordination sphere due to the presence of the Jahn-Teller effect, the expansion of the coordination sphere to six-coordination seems to provide a low-energy pathway for the reaction to take place.

The detachment of Tyr (step *a*), which is suggested in inhibition studies (Fig. 5 and [26, 29]), is accompanied by nucleophilic attack on the substrate (step *b*) by the coordinated hydroxide to form the *gem*-diolate transition state (B). Since the substrate may not form a coordination bond with the metal in the ES complex, a complete detachment of Tyr216 from the metal coordination sphere may take place only after or during nucleophilic attack on the substrate (steps *a* and *b*). The detachment of the coordinated Tyr may entitle the metal to “regain” its Lewis acidity for water activation, as reflected by a slight decrease in the  $\text{p}K_{a1}$  of the coordinated water in the  $k_{\text{cat}}$ -pH profile of the ES complex (Table 2). The transition state  $\text{ES}^\ddagger$  complex (B) is stabilized by the unbound Tyr via H-bonding to con-

tribute  $\sim 20 \text{ kJ mol}^{-1}$  stabilization energy, which is followed by bond cleavage and product release to complete the catalytic cycle. When the Tyr is completely deprotonated at high pH, it coordinates to the metal center and forms an inactive enzyme lacking the H-bonding stabilization at the stages A and B.

We report here a mechanistic study of the astacin-like metalloendopeptidase serralyisin by the use of metal-substitution, optical, and kinetic methods. A metal-centered mechanism has emerged, in which the coordinated hydroxide in the "metallotriad"  $\text{M}-\text{OH}\dots\text{Glu177}$  serves as the nucleophile and binding of Tyr216 to the metal is inhibitory. This mechanism may be applicable to the description of other astacin-like endopeptidases containing a coordinated Tyr. Moreover, the spectroscopically and magnetically accessible highly active Co- and Cu-serralyisin can serve as prototypes to provide further insight into the mechanistic roles of the coordinated water and the coordinated Tyr by the use of spectroscopic and magnetic resonance techniques. The high activity of Cu-serralyisin also suggests that the active site of this enzyme can serve as an ideal blueprint for the design of metal complexes in future studies of the emerging Cu-centered hydrolytic chemistry [45].

**Acknowledgements** Pavan Cheruvu and Reena Ninan, who participated in the University of South Florida Bio-Med and Life Sciences Summer Program, are acknowledged for their work on serralyisin purification and preliminary metal activation studies. The authors are also grateful for the support provided by the program and by the University.

## References

- Hooper NM (1994) FEBS Lett 354:1–6
- Rawlings ND, Barrett AJ (1993) Biochem J 290:205–218
- Jiang W, Bond JS (1992) FEBS Lett 312:110–114
- Murphy GJP, Murphy G, Reynolds JJ (1991) FEBS Lett 289:4–7
- Stöcker W, Grams F, Baumann U, Reinemer P, Gomis-Rüth F-X, McKay DB, Bode W (1995) Protein Sci 4:823–840
- Bond JS, Beynon RJ (1995) Protein Sci 4:1247–1261
- Dumermuth E, Sterchi EE, Jiang W, Wolz RL, Bond JS, Flannery AV, Beynon RJ (1991) J Biol Chem 266:21381–21385
- Sarras MP Jr (1996) BioEssays 18:439–442
- Gomis-Rüth F-X, Kress LF, Bode W (1993) EMBO J 12:4151–4157
- Baumann U (1994) J Mol Biol 242:244–251
- Baumann U, Wu S, Flaherty K, McKay D (1993) EMBO J 12:3357–3364
- Delepelaire P, Wandersman C (1989) J Biol Chem 264:9083–9089
- Bode W, Reinemer P, Huber R, Kleine T, Schnierer S, Tschesche H (1994) EMBO J 13:1263–1269
- Bode W, Gomis-Rüth F-X, Stöcker W (1993) FEBS Lett 331:134–140
- Zwilling R, Neurath H (1981) Methods Enzymol 80:633–665
- Stöcker W, Zwilling R (1995) Methods Enzymol 248:305–325
- Wolz RL, Bond JS (1995) Methods Enzymol 248:325–345
- Kessler E, Takahara K, Biniaminov L, Brusel M, Greenspan DS (1996) Science 271:360–362
- Shimell MJ, Ferguson EL, Childs ST, O'Conner MB (1991) Cell 67:469–481
- Yasumasu S, Yamada K, Akasada K, Mitsunaga K, Iuchi I, Shimada H, Yamagami K (1992) Dev Biol 153:250–258
- Yasumasu S, Iuchi I, Yamagami K (1994) Dev Growth Differ 36:241–250
- Lhomond G, Ghiglione C, Lepage T, Gache C (1996) Eur J Biochem 238:744–751
- Gomis-Rüth FX, Stöcker W, Huber R, Zwilling R, Bode W (1993) J Mol Biol 229:945–968
- Maeda H, Morihara K (1995) Methods Enzymol 248:395–413
- Hamada K, Hata Y, Katsuya Y, Hiramatsu H, Fujiwara T, Katsube Y (1996) J Biochem (Tokyo) 119:844–851
- Grams F, Dive V, Yiotakis A, Yiallourous I, Vassiliou S, Zwilling R, Bode W, Stöcker W (1996) Nat Struct Biol 3:671–675
- Baumann U, Bauer M, Letoffe S, Delepelaire P, Wandersman C (1995) J Mol Biol 248:653–661
- Mock WL, Yao J (1997) Biochemistry 36:4949–4958
- Park HI, Ming L-J (1998) J Inorg Biochem 72:57–62
- Yiallourous I, Berkhoff EG, Stöcker W (2000) FEBS Lett 484:224–228
- Kimura E (1994) Prog Inorg Chem 41:443–491
- Kimura E, Koike T (1997) Adv Inorg Chem 44:229–261
- Kimura E, Koike T, Toriumi K (1988) Inorg Chem 27:3687–3688
- Stöcker W, Sauer B, Zwilling R (1991) Biol Chem Hoppe-Seyler 372:385–392
- Miyoshi S, Shinoda SJ (1997) J Toxicol Toxin Rev 16:177–194
- Braun V, Schmitz G (1980) Arch Microbiol 124:55–61
- Matthews BW (1988) Acc Chem Res 21:333–340
- Christianson DW, Lipscomb WN (1989) Acc Chem Res 22:62–69
- Lipscomb WN, Sträter N (1996) Chem Rev 96:2375–2434
- Lyerly D, Kreger A (1979) Infect Immun 24:411–421
- Stöcker W, Wolz RL, Zwilling R, Strydom DJ, Auld DS (1988) Biochemistry 27:5026–5032
- Decedue CJ, Broussard EA II, Larson AD, Braymer HD (1979) Biochim Biophys Acta 569:293–301
- Cornish-Bowden A (1995) Fundamentals of enzyme kinetics, rev. edn. Portland, London
- Bertini I, Luchinat C (1994) In: Bertini I, Gray HB, Lippard SJ, Valentine JS (eds) Bioinorganic chemistry, chap 2. University Science Books, Sausalito, Calif
- Hegg EL, Burstyn JN (1998) Coord Chem Rev 173:133–165
- Frey ST, Murthy NN, Weintraub ST, Thompson LK, Karlin KD (1997) Inorg Chem, 36:956–957
- Frey ST, Sun HHJ, Murthy NN, Karlin KD (1996) Inorg Chim Acta 242:329–338
- Bayliss ME, Prescott MJ (1986) Biochemistry 25:8113–8117
- Bertini I, Luchinat C (1983) Met Ions Biol Syst 15:101–156
- Lin L-Y, Park HI, Ming L-J (1997) J Biol Inorg Chem 2:744–749
- Makinen MW, Wells GB, Kang S-O (1984) Adv Inorg Biochem 6:1–70
- Bertini I, Scozzafava A (1981) Met Ions Biol Syst 12:31–74
- Gomis-Rüth F-X, Grams F, Yiallourous I, Nar H, Küsthardt U, Zwilling R, Bode W, Stöcker W (1994) J Biol Chem 269:17111–17117
- Cleland WW (1982) Methods Enzymol 87:390–405
- Tipton KF, Dixon HB (1979) Methods Enzymol 63:183–234
- Cha J, Auld DS (1997) Biochemistry 36:16019–16024
- Cha J, Pedersen MV, Auld DS (1996) Biochemistry 35:15831–15838
- Mock WL, Stanford DJ (1996) Biochemistry 35:7369–7377
- Mock WL, Aksamawati M (1994) Biochem J 302:57–68
- Karplus PA, Pearson MA, Hausinger RP (1997) Acc Chem Res 30:330–337
- Auld DS, Vallee BL (1970) Biochemistry 9:4352–4359
- Izquierdo-Martin M, Stein RL (1992) J Am Chem Soc 114:325–331
- Brocklehurst K (1994) Protein Eng 7:291–299
- Rees DC, Lewis M, Honzatko RB, Lipscomb WN, Hardman KD (1981) Proc Natl Acad Sci USA 78:3408–3412

65. Bicknell R, Schäffer A, Bertini I, Luchinat C, Vallee BL, Auld DS (1988) *Biochemistry* 27:1050–1057
66. Bertini I, Donaire A, Messori L, Moratal J (1990) *Inorg Chem* 29:202–205
67. Ellis PD (1989) *J Biol Chem* 264:3108–3110
68. Borkakoti N, Winkler FK, Williams DH, D'Arcy A, Broadhurst MJ, Brown PA, Johnson WH, Murray EJ (1994) *Nat Struct Biol* 1:106–110
69. Bode W, Reinemer P, Huber R, Kleine T, Schnierer S, Tschesche H (1994) *EMBO J* 13:1263–1269